Coupled hydro-mechanical analysis of expansive soils
Parametric identification and calibration

Rawat, Abhishek ; Lang, Linzhi ; Baille, Wiebke; Dieudonné, Anne-Catherine; Collin, Frederique

DOI
10.1016/j.jrmge.2019.12.013

Publication date
2020

Document Version
Final published version

Published in
Journal of Rock Mechanics and Geotechnical Engineering

Journal of Rock Mechanics and Geotechnical Engineering 12 (2020) 620–629

Contents lists available at ScienceDirect

Journal of Rock Mechanics and Geotechnical Engineering

journal homepage: www.jrmge.cn

Full Length Article

Coupled hydro-mechanical analysis of expansive soils: Parametric identification and calibration

Abhishek Rawat [a,*], Linzhi Lang [a], Wiebke Baille [a], Anne-Catherine Dieudonne [b], Frederic Collin [c]

[a] Department of Foundation Engineering, Soil and Rock Mechanics, Ruhr-Universität Bochum, Universitätsstraße 150, 44780, Bochum, Germany
[b] Faculty of Civil Engineering and Geosciences, Delft University of Technology, Building 23, 2628 CN Delft, the Netherlands
[c] ArGEnCo, University of Liege, 4000 Liege, Belgium

ARTICLE INFO

Article history:
Received 5 April 2019
Received in revised form
12 October 2019
Accepted 5 December 2019
Available online 12 May 2020

Keywords:
Compacted bentonite
Backfill material
Deep geological repository
Constitutive modeling
Hydro-mechanical coupling
Water infiltration test

ABSTRACT

A methodology for identifying and calibrating the material parameters for a coupled hydro-mechanical problem is presented in this paper. For validation purpose, a laboratory-based water infiltration test was numerically simulated using finite element method (FEM). The test was conducted using a self-designed column-type experimental device, which mimicked the wetting process of a candidate backfill material in a nuclear waste repository. The real-time measurements of key state variables (e.g. water content, relative humidity, temperature, and total stresses) were performed with the monitoring sensors along the height of cylindrical soil sample. For numerical simulation, the modified Barcelona Basic Model (BBM) along with soil-water retention model for compacted bentonite was used. It shows that the identified model parameters successfully captured the moisture migration process under an applied hydraulic gradient in a bentonite-based compacted soil sample. A comparison between the measured and predicted values of total stresses both in axial and lateral directions along with other state variables revealed that heterogeneous moisture content was distributed along the hydration-path, resulting in non-uniform stress-deformation characteristics of soil.

1. Introduction

A compacted bentonite-sand mixture (50%:50% by dry mass) is generally proposed as a backfill material in the deep geological repositories in Germany for the final disposal of long-lived radioactive waste (e.g. Jobmann et al., 2015; Jobmann et al., 2017; Rothfuchs et al., 2005). The primary function of a backfill material is to limit advective water flow towards the waste canisters via available constructional gaps. The presence of bentonite in backfill materials fills such gaps when it comes in contact with water. Once these gaps are completely sealed with the bentonite, the material imposes swelling pressure on the roof and wall of disposal tunnel as a result of progressive hydration. Hence, the rate of saturation and the resulting swelling pressure are coupled with each other and it is a crucial coupling problem from the design point of view. Additionally, the mathematical formulation to reproduce this hydro-mechanical coupling is one of the major issues in the constitutive modeling for predicting the long-term behavior of backfill material. For this, several field and laboratory-based experimental and numerical investigations have been performed (e.g. Alonso et al., 2005; Martin and Barcala, 2005; Villar et al., 2005; Gens et al., 2009; Saba et al., 2014; Villar et al., 2014; Tripathy et al., 2015).

The Barcelona Basic Model (BBM) proposed by Alonso et al. (1990) is one of the most popular elastoplastic models. The model is an extension of the modified Cam-Clay model (MCCM) (Roscoe and Burland, 1968) for an unsaturated state. The model is suitable for predicting the mechanical behavior of collapsible soils and low to moderate expansive soils. Several modifications have been suggested in the original formulation of the BBM (e.g. Delahaye and Alonso, 2002; Vaunat and Gens, 2005; Sánchez et al., 2012; Sun and Sun, 2012; Zandarin et al., 2013; Gatabin et al., 2016) to reproduce the swelling potential of compacted bentonite-based materials. In general, the coupling between hydraulic and mechanical processes is introduced by incorporating the soil-water

* Corresponding author.
E-mail address: abhishek.rawat@rub.de (A. Rawat).
Peer review under responsibility of Institute of Rock and Soil Mechanics, Chinese Academy of Sciences.

https://doi.org/10.1016/j.jrmge.2019.12.013

retention model, which features the relationship between the soil suction and degree of saturation in the mechanical constitutive model (Sheng and Zhou, 2011).

In the last decade, several soil-water retention models have been proposed (e.g. Gallipoli et al., 2003; Sun et al., 2007; Nuth and Laloui, 2008; Tarantino, 2009; Mašín, 2010; Gallipoli, 2012), which correlate the air entry/air expulsion suction with the initial void ratio/dry density of soil samples. Based on the clay microstructural features in the compacted state, the double-structure water retention models have also been formulated (Romero and Vaunat, 2000; Della et al., 2015). Recently, Dieudonne et al. (2017) proposed a model to account for different water retention mechanisms in each structural level of a compacted bentonite. One of the major challenges when simulating coupled hydro-mechanical problems is the large number of model parameters. As a result, the model calibration and the parametric identification are not straightforward (Wheeler et al., 2002; Gallipoli et al., 2010; D'Onza et al., 2012; Gallipoli and D'Onza, 2013).

This paper presents a methodology for identifying and calibrating the material parameters for a fully coupled hydro-mechanical analysis using the modified BBM along with the soil-water retention model proposed by Dieudonne et al. (2017). For validating the identified model parameters, a laboratory-based water infiltration test was simulated using the finite element method (FEM) code LAGAMINE (Collin et al., 2002). The test was performed with a self-designed column-type experimental device, which facilitated the simultaneous measurements of water content, relative humidity, and the total stresses both in axial and lateral directions at various pre-selected locations during the hydration. The measured and predicted values of water content, relative humidity, axial and lateral stresses were compared, revealing that the identified model parameters successfully captured the moisture migration process in the compacted soil sample. The test results highlighted the key features of hydration-induced processes in unsaturated compacted expansive soils. The impact of moisture migration under an applied hydraulic gradient on the soil stiffness was found to be quite significant.

2. Materials

The Calcigel bentonite and medium sand (DIN18123, 2010) were used in this study. Table 1 summarizes the relevant geotechnical properties of the tested materials. The Calcigel bentonite contains 60%–70% montmorillonite and has the cation exchange capacity (CEC) of 740 mmol/kg with 67% of Ca^{2+} as a predominant exchangeable cation. For preparing a mixture of bentonite and sand (50%:50% by mass) with 9% initial moisture content, the required volume of distilled water was added to the oven-dried sand before mixing the Calcigel powder having 6% moisture content. The moist mixture was stored in sealed plastic bags for a period of 28 d.

Table 1
Soil properties used in this context.

Tested materials	Property	Value
Calcigel bentonite	Specific gravity	2.8
	Liquid limit (%)	119
	Plastic limit (%)	45
	Shrinkage limit (%)	10
	Plasticity index (%)	74
Sand	Specific gravity	2.65
	D_{10} (mm)	0.25
	D_{30} (mm)	0.4
	D_{60} (mm)	0.7
Bentonite-sand mixture (50%:50% by dry mass)	Specific gravity	2.725
	Liquid limit (%)	60
	Plastic limit (%)	32
	Plasticity index (%)	28

3. Methods

3.1. Column-type experimental device

A column-type experimental device was designed for investigating the coupled hydro-mechanical behavior of soils under an applied hydraulic gradient (Rawat et al., 2019). Fig. 1 shows the details of the designed experimental device. The technical details of the device can be found in Rawat et al. (2019). The monitoring instruments facilitate transient measurements of stresses both in axial and lateral directions along with the simultaneous measurements of temperature, water content and relative humidity at various pre-selected locations.

3.2. Preparation of soil sample

A cylindrical soil sample (diameter = 150 mm, and height = 300 mm) was assembled using three identical pre-compacted blocks (diameter = 150 mm, and height = 100 mm) of Calcigel bentonite-sand mixture having 9% moisture content. These blocks were prepared using uniaxial static compaction method by compacting the mixture into three layers. Each layer was subjected to vertical stress of 30 MPa in a specially designed cylindrical compaction mold (diameter = 150 mm, and height = 150 mm). It has a detachable base plate and a removable collar of 50 mm (in height). Once the compaction process was completed, the compacted block was removed from the mold. Further technical details concerning the compaction process in conjunction with the installation procedure of various monitoring sensors are provided in Rawat et al. (2019).

3.3. Water infiltration test

A test was performed by hydrating the soil sample from the bottom-end under a hydration pressure of 15 kPa in a controlled laboratory environment; the air outlet at top plug was kept open to evacuate the pore-air during saturation process. Effect of groundwater geochemistry on the clay–water interaction was not considered in this study, thus the distilled water was used to mimic the water ingress from the host rock. Monitoring sensors along with data logger continuously monitored relative humidity, temperature, water content, and total stresses both in axial and lateral directions. The test was performed for a period of 349 d. The post-experimental measurements (i.e. soil total suction and water content) were performed by collecting the soil samples from different locations along the height during dismantling of test set-up.

3.4. Numerical simulation

The water infiltration/wetting test was numerically analyzed using the FEM code LAGAMINE (Collin et al., 2002). The modified BBM (Alonso et al., 1990) along with the soil-water retention model proposed by Dieudonne et al. (2017) was used for this purpose. The proposed water retention model can consider different water retention mechanisms in each structural level, i.e. adsorption in intra-aggregate pores at microstructural level and capillarity in inter-aggregate pores at macrostructural level. The model was formulated in terms of water ratio (e_w), which is expressed as the sum of contributions from the water stored in micropores (e_{wm}) and the water in macropores (e_{wM}). The water stored in intra-aggregate pores is based on the Dubinin's adsorption theory (Dubinin and Radushkevich, 1947), which is expressed as

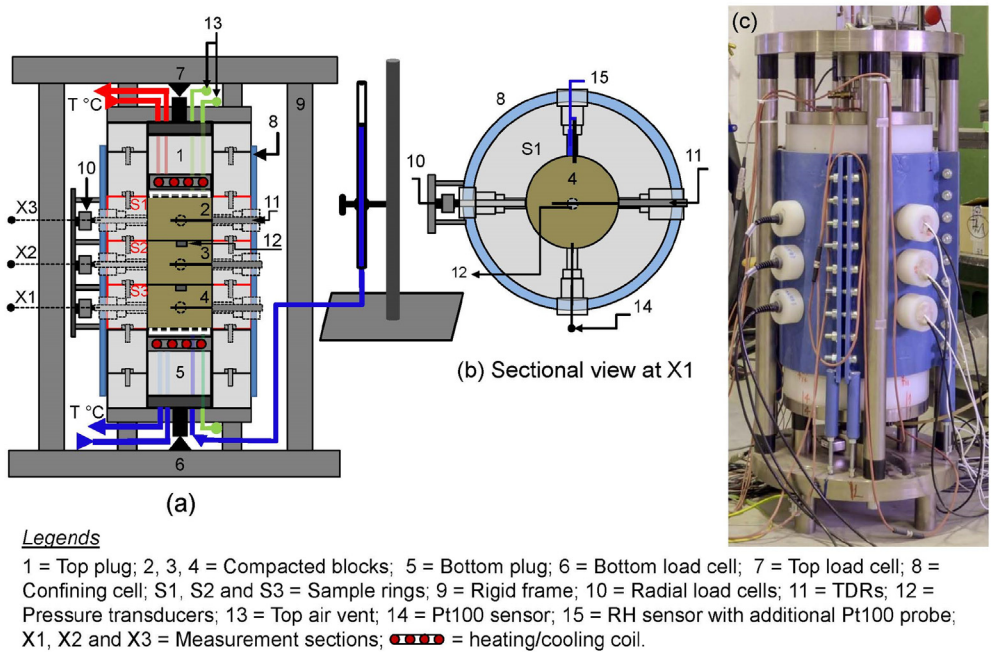

Fig. 1. Details of the self-designed column-type experimental set-up: (a) and (b) Vertical and horizontal sectional views, and (c) A photograph of the device (Rawat et al., 2019).

$$\Omega_{wm} = \Omega_m \exp\left\{ -\left[\frac{RT}{\beta_D E_0}\ln\left(\frac{\rho_v^0}{\rho_v}\right)\right]^{n_{ads}}\right\} \quad (1)$$

where Ω_{wm} is the volume of water adsorbed in the micropores at relative pressure ρ_v/ρ_v^0 and temperature T; Ω_m is the total volume of the micropores; R is the universal gas constant (= 8.314 J/mol·K); n_{ads} is the material parameter; β_D is the similarity constant; and E_0 is the characteristic energy of adsorption for a reference vapor for which $\beta_D = 1$.

Eq. (1) can be expressed in terms of water ratio by dividing both sides by volume of solid particles Ω_s as

$$e_{wm} = e_m \exp\left\{ -\left[\frac{RT}{\beta_D E_0}\ln\left(\frac{\rho_v^0}{\rho_v}\right)\right]^{n_{ads}}\right\} \quad (2)$$

where e_m is the microstructural void ratio.

Kelvin's equation (Edlefsen and Anderson, 1943) relates the relative vapor pressure in the soil pore volume with the soil total suction:

$$RH = \frac{\rho_v}{\rho_v^0} = \exp\left(\frac{-sM_w}{RT\rho_w}\right) \quad (3)$$

where RH is the relative humidity, M_w is the molecular mass of water (0.018 kg/mol), ρ_w is the density of water, and s is soil total suction.

By rearranging the constant parameters, the microstructural water retention domain can be expresses as

$$e_{wm} = e_m \exp[-(C_{ads}s)]^{n_{ads}} \quad (4)$$

where C_{ads} is the material parameter. The parameter n_{ads} controls the curvature of the water retention curve at the high suction values and C_{ads} is related to the original Dubinin's equation (Eq. (1)) through $\beta_D E_0$.

The microstructural void ratio (e_m) in the bentonite-based materials evolves during the hydration process. Dieudonne et al. (2017) adopted the microstructural evolution model (Eq. (5)) proposed by Della Vecchia et al. (2015) for calculating the structural changes of the material along with the water retention curve:

$$e_m = e_{m0} + \beta_0 e_w + \beta_1 e_w^2 \quad (5)$$

where e_{m0} is the microstructural void ratio for the dry material at $e_w = 0$; and β_0 and β_1 are the material parameters that quantify the swelling potential of the bentonite aggregates. In Eq. (5), it should be noted that for high dry density and high water content, it may lead to values of e_m higher than the total void ratio e. In this case, it is assumed that the microstructure is completely developed and then we have $e_m = e$.

The water stored in inter-aggregate pores (e_{wM}) is caused by capillarity:

$$e_{wM}(s, e, e_m) = (e - e_m)\left[1 + \left(\frac{s}{\alpha}\right)^n\right]^{-m} \quad (6)$$

where n and m are fitting parameters.

In order to feature the effect of macrostructural void ratio (e_M) on the air-entry suction value, the parameter α is introduced:

$$\alpha = \frac{A}{e - e_m} \quad (7)$$

where A is a parameter controlling the dependency of air-entry suction on the macrostructural void ratio (e_M).

The Kozney-Carman (KC) equation (Kozeny, 1927; Carman, 1938) along with the Mualem-van Genuchten equation (van Genuchten, 1980) provides a good estimate of deformation/stress-dependent hydraulic conductivity in unsaturated state during the transient hydration process. The original Kozeny-Carman formulation (Kozeny, 1927; Carman, 1938) did not consider the dual porosity domains in compacted bentonite. Thus the equation is

modified to incorporate the effect of change in the macrostructural void ratio (e_M) on the saturated hydraulic conductivity of soil:

$$K = K_0 \frac{(1-e_{M0})^M}{(e_{M0})^N} \frac{(e_M)^N}{(1-e_M)^M} \quad (8)$$

where K is the intrinsic permeability (m^2) for the compacted soil sample having macroscopic void ratio e_M; K_0 is the intrinsic permeability (m^2) for the reference macroscopic void ratio e_{M0}; and M and N are the fitting parameters.

4. Parametric identification and calibration

The procedure for identifying and calibrating the model parameters for a coupled hydro-mechanical analysis is presented herein. The model parameters can be grouped into three categories: (i) parameters related to the mechanical behavior of soil (BBM parameters), (ii) parameters related to the soil-water retention behavior (Dieudonne water retention model), and (iii) parameters related to the hydraulic behavior (saturated and unsaturated hydraulic conductivities).

4.1. Identification and calibration of BBM parameters

Suction-controlled oedometer tests were performed for identifying the BBM parameters. Tests were conducted using the high-pressure oedometer device. The bentonite-sand mixture (50%:50% by mass) having 9% initial water content was compacted directly inside the oedometer ring (diameter = 50 mm, and height = 15 mm) using uniaxial static compaction method. The achieved initial dry density was 1.8 Mg/m^3 similar to the compacted blocks in the water infiltration test. A total of four tests were performed (see Fig. 2). In the first test, the as-compacted sample (initial suction of 26.9 MPa) was subjected to one-dimensional (1D) compression-rebound stage. The other three tests were performed in two stages, i.e. suction-equilibrium stage and 1D compression-rebound stage. The vapor equilibrium technique (VET) was used to apply the desired suction level (i.e. 3.39 MPa or 10 MPa) in suction-equilibrium stage under 50 kPa vertical stress. As reduction in the soil total suction resulted in soil volumetric deformation, the change of the soil samples' height was continuously monitored during suction-equilibrium stage. Once the targeted suction-level was attained, the second stage, i.e. 1D compression-rebound, was initiated. For the test on saturated sample, the distilled water was supplied from the bottom-end under 50 kPa surcharge load prior to initiation of the second stage.

The original BBM (Alonso et al., 1990) was an extension of the MCCM by introducing the concept of hardening plasticity. Soil suction was considered as a hardening parameter signifying that the yield surface corresponding to MCCM expands with an increase in soil suction. The rate of expansion is represented by another yield surface known as the loading-collapse (LC) curve, which changes its position when the sample undergoes plastic deformation, whereas any combination of the net mean stress and soil suction ($p - s$) inside the elastic domain does not affect its position. Hence, it is essential that the sample should remain in the elastic domain during the suction-equilibrium stage. In this regard, the applied surcharge pressure should be kept lower than the expected swelling pressure of the compacted soil sample under constant volume condition, in order to ensure that the soil stress state (p, q, s) is within the elastic domain. In the present study, the sample was subjected to 50 kPa surcharge pressure and allowed to attain equilibrium with the applied suction level (i.e. 3.39 MPa or 10 MPa) under K_0 condition. The suction-controlled oedometer test results are shown in Fig. 3, along with the preconsolidation stress for saturated soil sample. It should be noted that the slope of unloading path for sample at 10 MPa suction applied is not shown in Fig. 3 due to the power failure during the test.

In the parametric analysis, three parameters ($\lambda(0)$, ω and r), which control the slope of normal compression lines at different suction levels were identified first. The results of oedometer test indicated that the collapse potential decreased with an increase in vertical net mean stress. On the other hand, Alonso et al. (1990) assumed that the slope of normal compression line would decrease when increasing the soil suction, based on the experimental results from García-Tornel (1988) on compacted low plastic kaolin and Maswoswe (1985) on compacted sandy clay. To overcome this problem that the collapse potential decreased with an increase in net stress, Wheeler et al. (2002) proposed a procedure for selecting suitable values of the model parameters r and p_c (reference stress). Following the procedure proposed by Wheeler

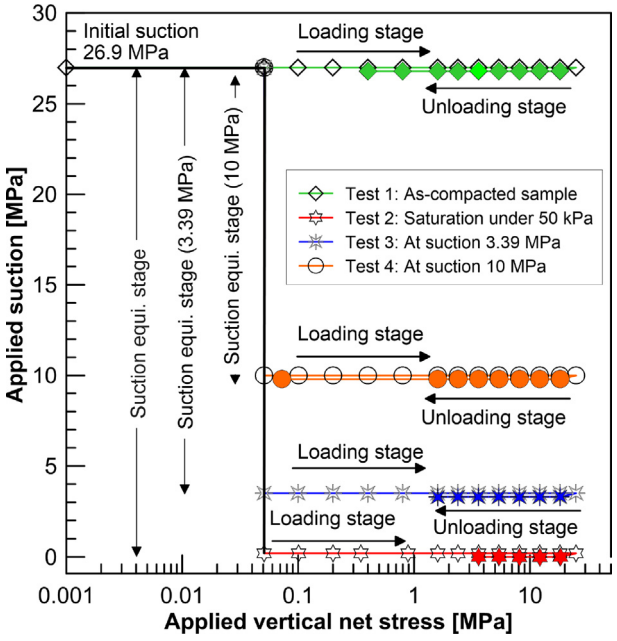

Fig. 2. Stress paths for suction-controlled oedometer tests.

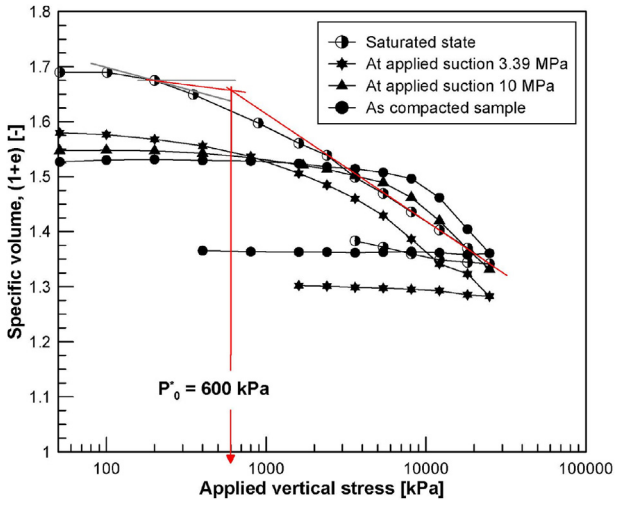

Fig. 3. Identification of the BBM parameters from suction-controlled oedometer tests.

et al. (2002), Fig. 4a shows the predicted variation of $\lambda(s)$ with soil suction.

In the second step, the model parameters related to the elastic behavior of soil (k and k_s) were identified. Fig. 4b presents the predicted variation of k with soil suction and the experimental values. It should be noted here that the fitting parameters in Fig. 4b were strongly affected by the elastic stiffness of soil in saturated condition ($s = 0$). For the slope of reversible wetting-drying line (k_s), the experimental data during suction-equilibrium stage (soil suction vs. specific volume) were used. Fig. 4c shows the variation of k_s with soil suction less than 50 kPa surcharge pressure. In the last step, the parameter p_c was selected to match the experimental data on preconsolidation stress values at different suction levels. Fig. 4d shows the LC curve for the compacted bentonite-sand mixture with the fitting parameters. Table 2 summarizes the BBM parameters for the Calcigel bentonite-sand mixture (50%:50% by mass).

Table 2
BBM parameters for compacted bentonite-sand mixture (50%:50% by dry mass).

Parameter		Value	Description
General	ϕ_0	0.34	Initial porosity
	ρ_s (kg/m^3)	2725	Solid density
	ψ_0 (MPa)	26.9	Initial suction
Plastic	$\lambda(0)$	0.082	Slope of normal compression line in saturated state
	p_0^* (MPa)	0.6	Preconsolidation pressure in saturated condition
	p^c (MPa)	3.6×10^3	Relative reference pressure
	r	1.491	First parameter defining the change in $\lambda(0)$ with suction
	ω (MPa^{-1})	0.1	Second parameter defining the change in $\lambda(0)$ with suction
Elastic	k_0	0.022	Initial elastic slope
	α_1 (MPa^{-1})	0.011	Parameter 1 related to elastic parameter
	α_2	−0.215	Parameter 2 related to elastic parameter
	G (MPa)	23.5	Shear modulus (for nonlinear elasticity)
	k_s	0.015	Slope of reversible wetting-drying line

4.2. Identification and calibration of soil-water retention model parameters

There are eight model parameters in formulation of double-structure water retention model proposed by Dieudonne et al. (2017), i.e.

(1) e_{m0}, β_0 and β_1 signify the evolution of the microstructural void ratio (e_m) with the water ratio (e_w);
(2) C_{ads} and n_{ads} control the water retention response of the intra-aggregate pores; and

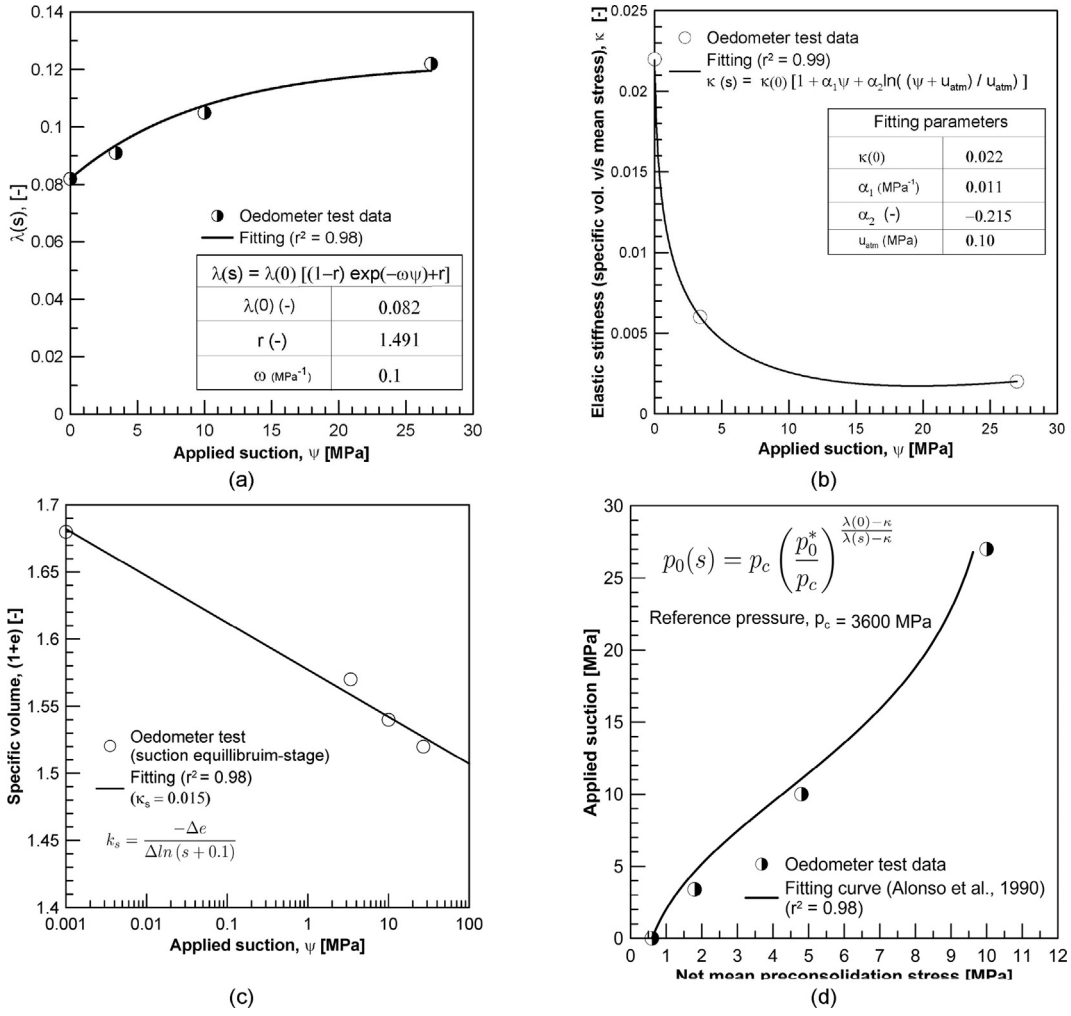

Fig. 4. Identification of the BBM parameters: (a) Slope of suction-dependent normal compression lines, (b) Applied net stress vs. specific volume at different applied suction levels, (c) Applied suction vs. specific volume at different applied net mean stresses; and (d) Loading-collapse curve.

(3) A, n and m govern the water retention behavior of the inter-aggregate retention region.

The model parameters (e_{m0}, β_0 and β_1) should be estimated first, independently of other parameters. It requires the pore size distribution (PSD) data of the compacted mixture of Calcigel bentonite-sand (50%:50% by mass) at different water ratios (e_{m0}). Additionally, the identification of e_{m0} requires the PSD data of the oven-dried sample, i.e. water void ratio $e_w = 0$. Agus (2005) obtained the PSD data from mercury intrusion porosimetry (MIP) tests on the samples having an identical water ratio (i.e. $e_w = 0.245$). The MIP tests were conducted for the as-compacted, oven-dried and swollen samples. To quantify the microstructural and macrostructural void ratios from the PSD data, the delimiting pore sizes were identified by drawing tangents on the cumulative intrusion curves for as-compacted (0.05 μm), swollen (0.02 μm) and oven-dried (0.02 μm) samples, as shown in Fig. 5.

The MIP test data for the as-compacted samples revealed that the intra-aggregate or micropore volume was 59%, while the inter-aggregate pore volume was 41% of the total pore volume. For the oven-dried samples, the intra-aggregate and inter-aggregate pore volumes were 55% and 45% of the total pore volume, respectively. For the swollen samples, the intra-aggregate and inter-aggregate pore volumes were 57% and 43% of the total pore volume, respectively. Based on the above MIP test data, the corresponding microstructural and macrostructural void ratio were obtained for as-compacted samples ($e_m = 0.3$ and $e_M = 0.21$ for $e_w = 0.245$), oven-dried samples ($e_{m0} = 0.25$ and $e_M = 0.2$ for $e_w = 0$) and swollen samples ($e_{m0} = 0.45$ and $e_M = 0.35$ for $e_w = 0.8$). Fig. 6 shows the evolution of microstructural void ratio with water ratio, and the obtained data were fitted with the model proposed by Della Vecchia et al. (2015).

It is clear that the model parameters C_{ads} and n_{ads} control the soil-water retention behavior of intra-aggregate or micropores. The identification of these parameters requires sorption/wetting tests under constant volume condition on the compacted samples having different initial dry densities. In the present study, the compacted samples (initial dry density of 1.8 Mg/m^3) were subjected to wetting under a constant volume condition, while the data for samples of 2 Mg/m^3 were collected from Agus (2005). The soil-water retention behavior at higher suction level was governed by the intra-aggregate or micropores and did not depend on the sample initial state. The parameter C_{ads} controlled the slope of soil-water retention curve at higher suction value and varied in 0.018–0.0018 MPa^{-1} (Dieudonne et al., 2017). The parameter n_{ads} controlled the curvature of water retention curve in the high suction range and could be treated as a fitting parameter.

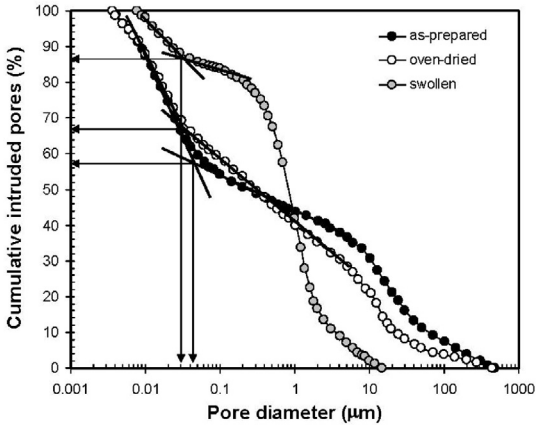

Fig. 5. Determination of micropores and macropores from the PSD data from Agus (2005).

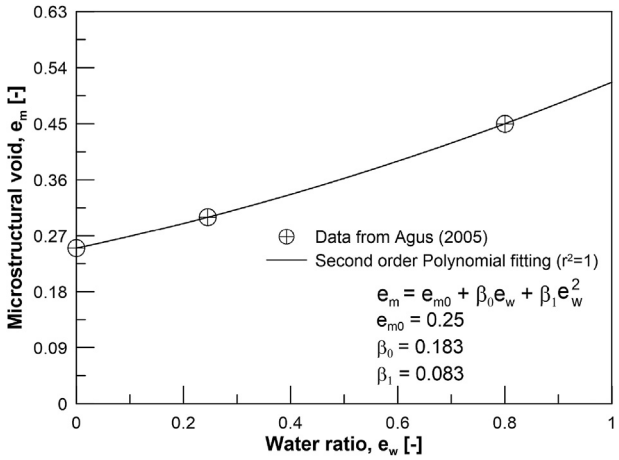

Fig. 6. Evolution of microstructural void ratio with water void ratio for compacted Calcigel bentonite-sand mixture (50%:50% by mass) from Agus (2005).

The macrostructural water retention model parameters A, n and m were identified using the sorption/wetting tests data for soil samples having different initial dry densities (i.e. 1.8 Mg/m^3 and 2 Mg/m^3). The macroscopic parameter (A) captured the dependency of air-entry (or air-occlusion) suction on the initial void ratio. The parameters n and m controlled the drying-wetting rate of materials in low suction range. Fig. 7 shows the calibration of Dieudonne water retention model and the van Genuchten model against the experimental data.

4.3. Identification and calibration of hydraulic parameters

The parametric identification for Kozeny-Carman (Carman, 1938; Kozeny, 1927) formulation (Eq. (9)) requires the intrinsic permeability values of saturated soil samples having different initial porosities. The intrinsic permeability (m^2) of material is related to the saturated hydraulic conductivity (m/s) of material.

$$K = K_0 \frac{(1-\phi_0)^m}{\phi_0^n} \frac{\phi^n}{(1-\phi)^m} \tag{9}$$

where K is the intrinsic permeability (m^2) of material with porosity ϕ, K_0 is the intrinsic permeability (m^2) of material with reference

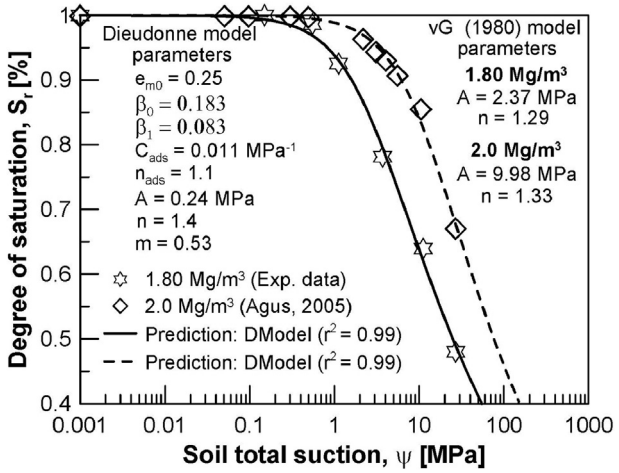

Fig. 7. Calibration of soil water retention model against the experimental data on Calcigel bentonite-sand mixture (50%:50% by mass) at two different dry densities (wetting path under confined condition).

porosity ϕ_0, and m and n are the fitting parameters. The saturated permeability can be written as

$$k_f = \frac{K_f \rho_f g}{\mu_f} \tag{10}$$

where k_f is the saturated permeability (m/s), K_f is intrinsic permeability (m^2), ρ_f is the density of fluid (kg/m^3), g is the gravitational acceleration (m/s^2), and μ_f is the dynamic viscosity of fluid (Pa s).

The saturated hydraulic conductivity values at different initial dry densities of the Calcigel bentonite-sand mixture (50%:50% by mass) were collected from the literature (Agus, 2005; Long, 2014). For an initial dry density of 1.8 Mg/m^3, the saturated hydraulic conductivity of the compacted mixture was determined by the oedometer test. The collected and measured saturated permeability data with the Kozeny-Carman model parameters for the investigated material are shown in Fig. 8. For the relative permeability in unsaturated state, a closed-form equation proposed by van Genuchten (1980) was used. The parameter λ was calibrated by best fitting the response of three relative humidity sensors located at 50 mm, 150 mm and 250 mm from the bottom-end. Table 3 summarizes the water retention model and the hydraulic parameters.

5. Numerical analysis of water infiltration test

The model geometry along with the initial boundary conditions used in the numerical simulation is shown in Fig. 9. The model dimensions were determined according to the sample size in the water infiltration test (75 mm along *X*-axis and 300 mm along *Y*-axis). The initial stress in the material was assumed to be atmospheric (0.1 MPa and isotropic). The temperature in this study was kept constant at 20 °C. The initial total suction of the material was assigned to 26.9 MPa. For initiating the hydration, the liquid pressure at the bottom nodes was changed by a hydration pressure of 15 kPa.

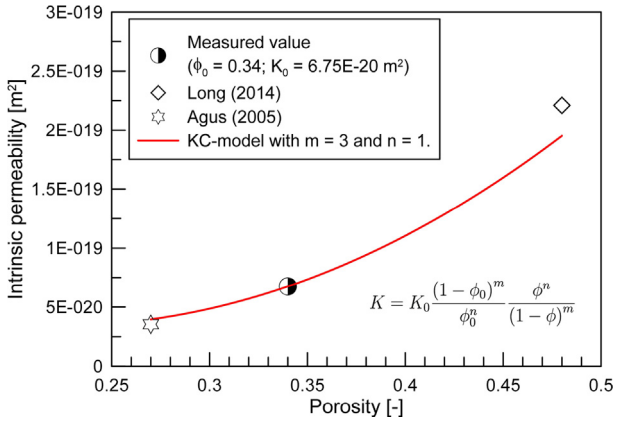

Fig. 8. Sample initial porosity vs. intrinsic permeability: Experimental data and predicted values using Kozeny-Carman formulation.

Table 3
Model parameters for hydraulic behavior of compacted bentonite-sand mixture (50%:50% by mass).

Parameter	Value	Note
e_{m0}	0.25	For the microstructural water retention domain (Dieudonne et al., 2017)
β_0	0.183	
β_1	0.083	
C_{ads} (MPa^{-1})	1.1×10^{-2}	
n_{ads}	1.1	
A (MPa)	0.24	For the macrostructural water retention domain (Dieudonne et al., 2017)
m	0.53	
n	1.4	
K_0 (m^2)	6.75×10^{-20}	For Kozney-Carman formulation
K (m^2)	–	
m	3	
n	1	
λ	0.5	Relative permeability (water/air)

6. Results and discussion

6.1. Rate of saturation during hydration phase

Fig. 10a,b shows a comparison between the predicted vs. observed relative humidity and water content evolution along the hydration path with the measured post-experimental values. It shows that the distance to the hydration-end significantly affected the rate of saturation. As a result, the water content increased rapidly at section X1. The predicted values showed a good agreement with the measured ones; however, the predicted values of water content were slightly higher than the measured ones at farther sections (i.e. X2 and X3).

Fig. 11 compares the predicted, calculated and measured infiltrated water volumes during the hydration process. The calculated values were deduced from the measurements of transient water content. The predicted values show a good agreement with the measured and calculated ones. A decrease in the flow rate with elapsed time was observed, which signified the effect of soil suction gradient on the rate of saturation.

6.2. Development of stresses due to wetting process

The clay–water interaction in terms of either sorption (wetting) or desorption (drying) of bentonite results in volumetric deformation (swelling or shrinkage, respectively). The sorption or wetting of compacted bentonite under confined conditions generates swelling pressure, which acts against the confinement. During the water infiltration test, the swelling pressure was measured both in axial and lateral directions. The predicted values obtained from the numerical analysis were compared with the measured ones (Fig. 12 in axial direction and Fig. 13 in lateral direction).

Fig. 12 presents the predicted and measured axial total stress values at the top- and bottom-end of a cylindrical soil sample. In the water infiltration test, the hydration was initiated from the bottom-end, and the top load cell measured the swelling pressure exerted from the bottom elements due to wetting. For frictionless cell boundaries between the soil sample and test cell, the measured axial stresses at two extreme ends should be the same in case of hydration under a confined condition. On the other hand, the measured axial stress values at the top- and bottom-end were dissimilar. This dissimilarity in the measured axial stresses may be due to some reasons, such as (i) dissimilar compressibility characteristics along the hydration-path due to the non-homogeneous moisture distribution, (ii) presence of construction joints meant for installing the pressure transducers, (iii) side frictional resistance between the sample and the PVDF (Polyvinylidene fluoride) rings, and (iv) composite nature of the sample due to the presence of sensors that created complex stress-deformation characteristics of the system. These features were not considered explicitly during the simulation. A decent agreement was observed between the predicted and measured axial total stress data at the bottom-end; however, the predicted values were slightly higher than the measured ones.

In the numerical analysis of water infiltration test under a confined condition, the elastic strain according to the BBM is given:

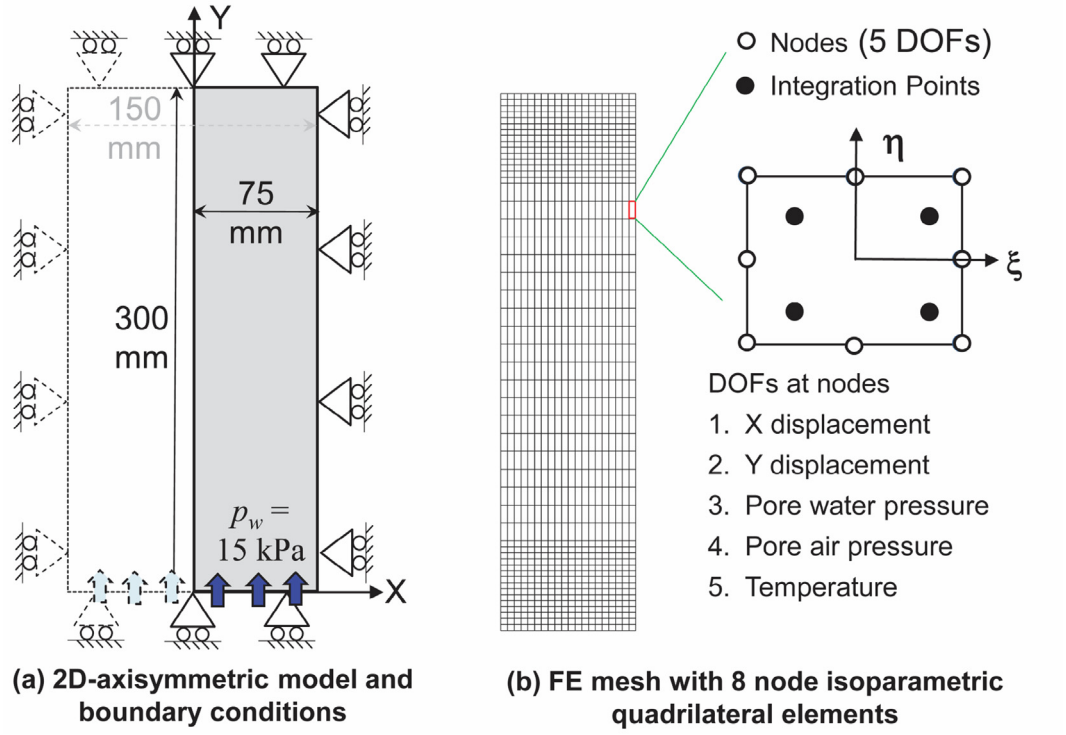

Fig. 9. Finite element simulation of water infiltration test: Features of numerical analysis.

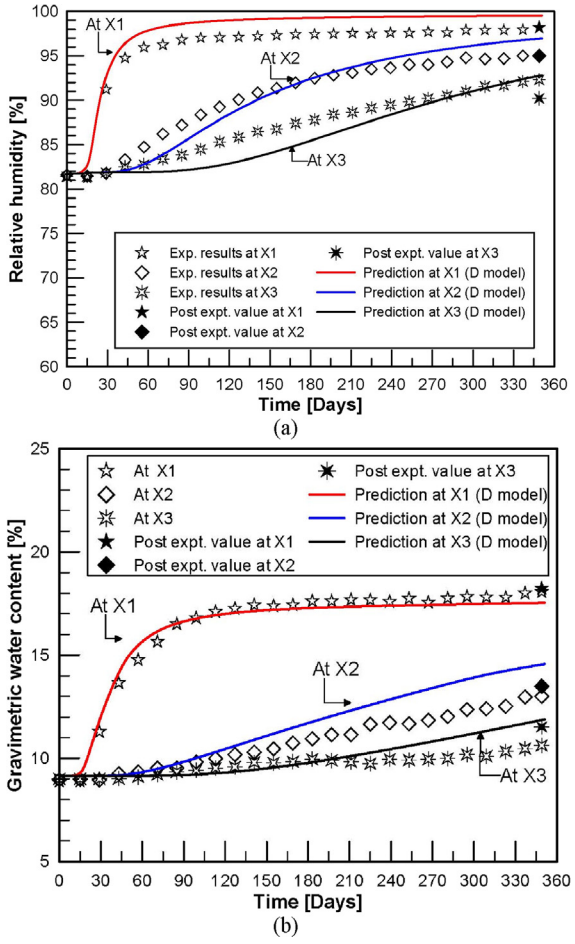

Fig. 10. Rate of saturation during transient hydration process: Measured vs. predicted values of (a) Relative humidity, and (b) Water content evolution.

$$d\varepsilon_v^e = d\varepsilon_{vp}^e + d\varepsilon_{vs}^e = \frac{k}{1+e}\frac{dp}{p} + \frac{k_s}{1+e}\frac{ds}{s+u_{atm}} = \frac{dp}{K} + \frac{ds}{K_s} \tag{11}$$

For hydration under confined conditions, we have

$$d\varepsilon_v^e = 0 \tag{12}$$

$$d\varepsilon_{vp}^e = -d\varepsilon_{vs}^e \tag{13}$$

$$\frac{k}{1+e}\frac{dp}{p} = -\frac{k_s}{1+e}\frac{ds}{s+u_{atm}} \tag{14}$$

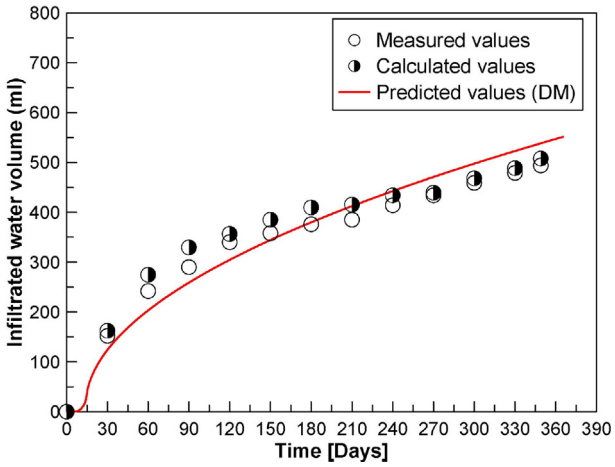

Fig. 11. Comparison between measured and predicted values: Infiltrated water volume over elapsed time.

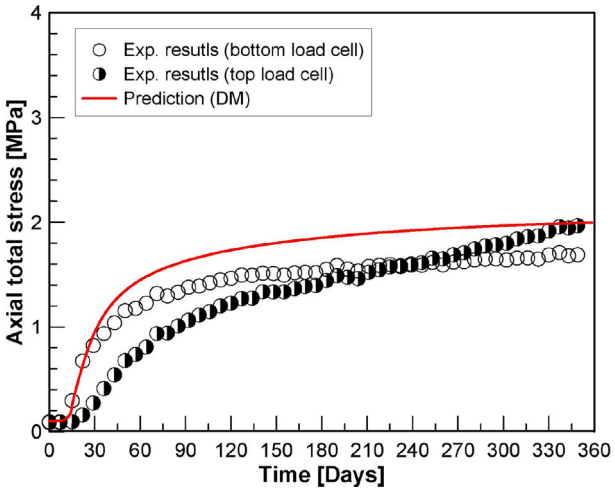

Fig. 12. Development of swelling pressure in axial direction due to wetting under confined conditions: Measured vs. predicted values.

$$dp = -\frac{k_s}{k}\frac{ds}{(s+u_{atm})}p \tag{15}$$

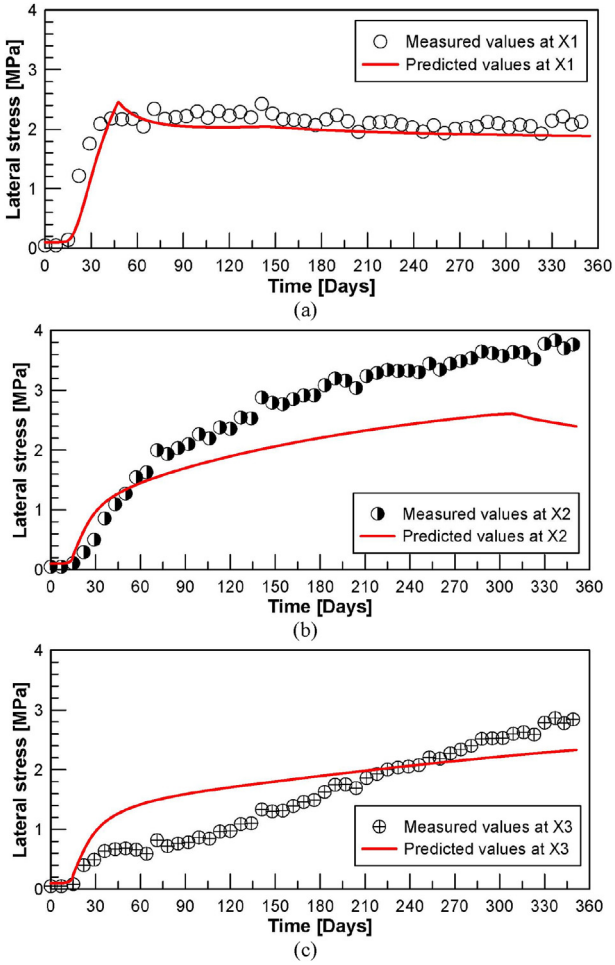

Fig. 13. Development of swelling pressure in lateral direction due to wetting under confined conditions: Measured vs. predicted values. (a) At section X1 (50 mm from bottom-end); (b) At section X2 (150 mm from bottom-end); (c) At section X3 (250 mm from bottom-end).

By integrating Eq. (15), the increase in mean stress p with suction s within the elastic domain can be expressed as

$$p(s) = p_0\left(\frac{s_0+u_{atm}}{s+u_{atm}}\right)^{\frac{k_s}{k}} \tag{16}$$

where p_0 and s_0 are the initial mean net stress and soil suction, respectively.

Eqs. (15) and (16) reveal that the incremental change in mean stress in the elastic domain depends on the ratio of elastic stiffness (k_s/k), incremental change in suction (ds) and the soil stress state (p, s). Fig. 13 presents a comparison between the predicted and measured values of lateral total stress along the height of soil sample. With initiation of hydration, the measured total stress at the section X1 increased quickly and reached 2.18 MPa within 45 d. With further hydration, the measured values at the section X1 showed some oscillations before reaching a value of 2.13 MPa in 349 d. The model predictions showed a good agreement with the measured data at section X1; however, the predicted values disagree with the measured data at sections X2 and X3. In general, the stress-deformation characteristics of a compacted bentonite-based soil sample during hydration from one end involves various complex processes, which includes swelling of soil layers, hydration-induced heterogeneity along the height of soil sample, and interaction between different soil layers. Also, the presence of technical gaps and non-uniform soil stiffness in axial and lateral directions are responsible for a different axial and lateral swelling pressure response.

7. Concluding remarks

The present study investigated the coupled hydro-mechanical behavior of a compacted bentonite-sand mixture (50%:50% by mass). A water infiltration test was conducted to mimic the transient hydration process of a candidate backfill material in nuclear waste repository. The test was conducted using a column-type experimental device. Later, the water infiltration test was numerically simulated using FEM. In the numerical analysis, the modified BBM along with the double-structure water retention model was used. For identifying the model parameters, a methodology was proposed using conventional laboratory-based experiments on the elementary soil samples. To validate the identified model parameters, the predicted values from the numerical analysis were compared with the measured ones. The experimental results revealed the moisture migration along the height of unsaturated soil sample under an applied hydraulic gradient. The double-structure water retention model proposed by Dieudonne et al. (2017) successfully captured the moisture migration process in the compacted soil sample.

The axial and lateral total stress measurements during the water infiltration highlighted the consequences of a heterogeneous moisture distribution in compacted bentonite-based materials. A comparative analysis of the measured and predicted total stress values along the height of soil sample signified the role of interfacial friction between the soil sample and cell-wall and anisotropic swelling behavior, which provided the key inputs to improve the existing constitutive models for a coupled hydro-mechanical analysis.

Declaration of Competing Interest

The authors wish to confirm that there are no known conflicts of interest associated with this publication and there has been no

significant financial support for this work that could have influenced its outcome.

Acknowledgments

The authors are grateful to the German Research Foundation (DFG) for the financial support (Grant No. SCHA 675/17-1).

References

Agus SS. An experimental study on hydro-mechanical characteristics of compacted bentonite-sand mixtures. PhD Thesis. Weimar, Germany: Bauhaus-University Weimar; 2005.
Alonso EE, Gens A, Josa A. A constitutive model for partially saturated soils. Géotechnique 1990;40(3):405–30.
Alonso EE, Alcoverro J, Coste F, Malinsky L, Merrien-Soukatchoff V, Kadiri I, Nowak T, Shao H, Nguyen TS, Selvadurai APS, et al. The FEBEX benchmark test: case definition and comparison of modelling approaches. International Journal of Rock Mechanics and Mining Sciences 2005;42(5–6):611–38.
Carman PC. Fundamental principles of industrial filtration (a critical review of present knowledge). Transaction of the Institute of Chemical Engineers 1938;16:168–88.
Collin F, Li XL, Radu JP, Charlier R. Thermo-hydro-mechanical coupling in clay barriers. Engineering Geology 2002;64(2–3):179–93.
Delahaye CH, Alonso E. Soil heterogeneity and preferential paths for gas migration. Engineering Geology 2002;64(2–3):251–71.
Della Vecchia G, Dieudonné AC, Jommi C, Charlier R. Accounting for evolving pore size distribution in water retention models for compacted clays. International Journal for Numerical and Analytical Methods in Geomechanics 2015;39:702–23.
Dieudonne AC, Della Vecchia G, Charlier R. Water retention model for compacted bentonites. Canadian Geotechnical Journal 2017;54(7):915–25.
DIN18123. Soil, Investigation and testing—determination of grain-size distribution. Berlin: German Institute for Standardisation; 2010.
D'Onza F, Gallipoli D, Wheeler SJ. A new procedure for determining parameter values in the Barcelona Basic Model. In: Unsaturated soils: research and applications. Berlin: Springer; 2012. p. 93–102.
Dubinin MM, Radushkevich LV. The equation of the characteristic curve of the activated charcoal. In: Proceedings of the union of soviet socialist republics academy of sciences. Moscow; 1947. p. 331–7.
Edlefsen N, Anderson A. Thermodynamics of soil moisture. Hilgardia 1943;15(2):31–298.
Gallipoli D, Gens A, Sharma R, Vaunat J. An elasto-plastic model for unsaturated soil incorporating the effects of suction and degree of saturation on mechanical behaviour. Géotechnique 2003;53(1):123–35.
Gallipoli D, D'Onza F, Wheeler SJ. A sequential method for selecting parameter values in the Barcelona Basic Model. Canadian Geotechnical Journal 2010;47(11):1175–86.
Gallipoli D. A hysteretic soil-water retention model accounting for cyclic variations of suction and void ratio. Géotechnique 2012;62(7):605–16.
Gallipoli D, D'Onza F. Calibration of elasto-plastic models for unsaturated soils under isotropic stresses. Engineering Geology 2013;165:64–72.
García-Tornel AJ. Un modelo elastoplástico para suelos no saturados. PhD Thesis. Barcelona, Spain: Universitat Politècnica de Catalunya; 1988 (in Spanish).
Gatabin C, Talandier J, Collin F, Charlier R, Dieudonné A-C. Competing effects of volume change and water uptake on the water retention behaviour of a compacted MX-80 bentonite/sand mixture. Applied Clay Science 2016;121–122:57–62.
Gens A, Sánchez M, Guimarães LDN, Alonso E, Lloret A, Olivella S, Villar M, Huertas F. A full-scale in situ heating test for high-level nuclear waste disposal: observations, analysis and interpretation. Géotechnique 2009;59(4):377–99.
Jobmann M, Flügge J, Hammer J, Herold P, Krone J, Kühnlenz T, Li S, Lommerzheim A, Meleshyn A, Wolf J. Site-specific evaluation of safety issues for high-level waste disposal in crystalline rocks. Technical Report No. TEC-28-2015-AB. 2015.
Jobmann M, Flügge J, Gazul R, Hammer J, Herold P, Krone J, Kuate Simo E, Kühnlenz T, Laggiard E, Lommerzheim A, Meleshyn A, Müller C, Rübel A, Wolf J, Zhao H. Investigation on long-term safety aspects of a radioactive waste repository in a diagenetic clay formation. Technical Report No. TEC-32-2016-AB. 2017.
Kozeny J. Über kapillare Leitung des Wassers im Boden Aufstieg, Versickerung und Anwendung auf die Bewässerung, 136. Sitzb. Akad. Wiss. Wien. Math. naturw. Klasse; 1927 (in German).
Long N-T. Coupled thermo-hydro-mechanical analysis: experiment and back analysis. PhD Thesis. Bochum, Germany: Ruhr-Universität Bochum; 2014.
Mašín D. Predicting the dependency of a degree of saturation on void ratio and suction using effective stress principle for unsaturated soils. International Journal for Numerical and Analytical Methods in Geomechanics 2010;34(1):73–90.
Martin P, Barcala J. Large scale buffer material test: mock-up experiment at CIEMAT. Engineering Geology 2005;81(3):298–316.
Maswoswe J. Stress paths for compacted soil during collapse due to wetting. PhD Thesis. London, UK: Imperial College London; 1985.
Nuth M, Laloui L. Advances in modelling hysteretic water retention curve in deformable soils. Computers and Geotechnics 2008;35(6):835–44.
Rawat A, Baille W, Tripathy S. Swelling behavior of compacted bentonite-sand mixture during water infiltration. Engineering Geology 2019;257:105–41.
Romero E, Vaunat J. Retention curves of deformable clays. In: Experimental evidence and theoretical approaches in unsaturated soils. Boca Raton, USA: CRC Press; 2000. p. 91–106.
Roscoe KH, Burland JB. On the generalised stress-strain behaviour of wet clay. Engineering Plasticity 1968:535–609.
Rothfuchs T, Jockwer N, Miehe R, Zhang CL. Self-sealing barriers of clay/mineral mixtures in a clay repository: SB experiment in the Mont Terri Rock Laboratory. Technical Report No. GRS-212 (ISBN 3-931995-79-8). Gesellschaft für Anlagen- und Reaktorsicherheit (GRS); 2005.
Saba S, Cui YJ, Barnichon JD, Tang AM. Investigation of the swelling behaviour of compacted bentonite–sand mixture by mock-up tests. Canadian Geotechnical Journal 2014;51(12):1399–412.
Sánchez M, Gens A, Olivella S. THM analysis of a large-scale heating test incorporating material fabric changes. International Journal for Numerical and Analytical Methods in Geomechanics 2012;36(4):391–421.
Sheng D, Zhou A-N. Coupling hydraulic with mechanical models for unsaturated soils. Canadian Geotechnical Journal 2011;48(5):826–40.
Sun D, Sheng D, Sloan SW. Elastoplastic modelling of hydraulic and stress–strain behaviour of unsaturated soils. Mechanics of Materials 2007;39(3):212–21.
Sun W, Sun D. Coupled modelling of hydro-mechanical behaviour of unsaturated compacted expansive soils. International Journal for Numerical and Analytical Methods in Geomechanics 2012;36(8):1002–22.
Tarantino A. A water retention model for deformable soils. Géotechnique 2009;59(9):751–62.
Tripathy S, Thomas HR, Bag R. Geoenvironmental application of bentonites in underground disposal of nuclear waste: characterization and laboratory tests. Journal of Hazardous, Toxic, and Radioactive Waste 2015;21(1):D4015002.
van Genuchten MT. A closed-form equation for predicting the hydraulic conductivity of unsaturated soils. Soil Science Society of America Journal 1980;44(5):892–8.
Vaunat J, Gens A. Analysis of the hydration of a bentonite seal in a deep radioactive waste repository. Engineering Geology 2005;81(3):317–28.
Villar M, Campos R, Gutiérrez-Nebot L. Long-term performance of engineered barrier systems PEBS. EB experiment laboratory post-mortem analyses report, the seventh framework programme of the European atomic energy community (Euratom). DELIVERABLE 2014. D2:1–7.
Villar MV, García-Siñeriz JL, Bárcena I, Lloret A. State of the bentonite barrier after five years operation of an in situ test simulating a high level radioactive waste repository. Engineering Geology 2005;80(3–4):175–98.
Wheeler SJ, Gallipoli D, Karstunen M. Comments on use of the Barcelona basic model for unsaturated soils. International journal for numerical and analytical methods in Geomechanics 2002;26(15):1561–71.
Zandarin MT, Alonso E, Olivella S. A constitutive law for rock joints considering the effects of suction and roughness on strength parameters. International Journal of Rock Mechanics and Mining Sciences 2013;60:333–44.

Dr. Abhishek Rawat has recently completed his PhD degree (2014–2019) from Ruhr University Bochum, Germany in Geotechnical Engineering. Prior to joining PhD, he was working as a Scientific Officer at Bhabha Atomic Research Centre Mumbai from 2009 to 2014. During this period, he was associated with the Indian Deep Geological Repository Program for the permanent disposal of high-level radioactive waste. He did MSc from IIT Bombay from 2007 to 2009 in Geotechncial Engineering. His main research area is the application-based phenomenological soil testing approach for unsaturated soils particularly relevant to nuclear waste disposal.